Proc. Natl. Acad. Sci. USA
Vol. 86, pp. 1689–1693, March 1989
Neurobiology

Blocking and isolation of a calcium channel from neurons in mammals and cephalopods utilizing a toxin fraction (FTX) from funnel-web spider poison

(ion-channel blocker/Purkinje cell/squid synapse)

R. LLINÁS, M. SUGIMORI, J.-W. LIN, AND B. CHERKSEY

Department of Physiology and Biophysics, New York University Medical School, New York, NY 10016

Contributed by R. Llinás, November 22, 1988

ABSTRACT **A Ca^{2+}-channel blocker derived from funnel-web spider toxin (FTX) has made it possible to define and study the ionic channels responsible for the Ca^{2+} conductance in mammalian Purkinje cell neurons and the preterminal in squid giant synapse. In cerebellar slices, FTX blocked Ca^{2+}-dependent spikes in Purkinje cells, reduced the spike afterpotential hyperpolarization, and increased the Na^{+}-dependent plateau potential. In the squid giant synapse, FTX blocked synaptic transmission without affecting the presynaptic action potential. Presynaptic voltage-clamp results show blockage of the inward Ca^{2+} current and of transmitter release. FTX was used to isolate channels from cerebellum and squid optic lobe. The isolated product was incorporated into black lipid membranes and was analyzed by using patch-clamp techniques. The channel from cerebellum exhibited a 10- to 12-pS conductance in 80 mM Ba^{2+} and 5–8 pS in 100 mM Ca^{2+} with voltage-dependent open probabilities and kinetics. High Ba^{2+} concentrations at the cytoplasmic side of the channel increased the average open time from 1 to 3 msec to more than 1 sec. A similar channel was also isolated from squid optic lobe. However, its conductance was higher in Ba^{2+}, and the maximum opening probability was about half of that derived from cerebellar tissue and also was sensitive to high cytoplasmic Ba^{2+}. Both channels were blocked by FTX, Cd^{2+}, and Co^{2+} but were not blocked by ω-conotoxin or dihydropyridines. These results suggest that one of the main Ca^{2+} conductances in mammalian neurons and in the squid preterminal represents the activation of a previously undefined class of Ca^{2+} channel. We propose that it be termed the "P" channel, as it was first described in Purkinje cells.**

While different Ca^{2+}-channel blockers have been described in past years (1), a true blocker for the main Ca^{2+}-dependent action potential in mammalian and in some molluscan neurons had not been encountered. This lack of a suitable blocker suggested that at least one of the main Ca^{2+} conductances present in the central nervous system (CNS) does not belong to the categories proposed by Tsien and co-workers (2, 3), as those channels respond quite specifically to dihydropyridines and ω-conotoxins. The use of funnel-web spider toxin (FTX) as a CNS Ca^{2+}-channel blocker was first described in Purkinje cells, where it blocked dendritic spiking (4). At that time the fragment utilized was known as AG1 and was obtained from Bioactives (Salt Lake City, UT). Because of the variability in the blocking observed, we attempted to isolate the main factor involved in this blockage from crude venom. We report here on the specific neuronal Ca^{2+}-channel blocking properties of FTX and its use in the isolation of functional channels, which we have studied in the black lipid membranes. That the Ca^{2+}-channel blocking fraction, which we call FTX, is different from that initially described as AG1 relates to its molecular mass as determined chromatographically, which is one-fifth that of AG1, and its high affinity for Ca^{2+} conductance both in the mammalian CNS and the squid giant synapse. Some of these results have been presented as short communications (4–7).

The publication costs of this article were defrayed in part by page charge payment. This article must therefore be hereby marked "*advertisement*" in accordance with 18 U.S.C. §1734 solely to indicate this fact.

MATERIALS AND METHODS

Electrophysiological Techniques. The methods utilized for the brain slice work on the cerebellum and for the giant synapse are the same as those described in previous papers from our laboratory (8, 9). Purkinje cell recordings were obtained from *in vivo* adult guinea pig cerebellar slices. These cells were impaled at either the soma or the dendrites. Electrical excitability of the cell was determined by direct stimulation of the neurons. Sodium conductances were blocked by using tetrodotoxin (TTX).

The experiments on the squid (*Loligo Pealeii*) giant synapse were performed at the Marine Biological Laboratory (Woods Hole, MA). Pre- and postsynaptic recordings from the giant synapse were utilized to test the action of FTX on synaptic transmission, and presynaptic voltage-clamp was used to determine the effect of the toxin fraction on the inward presynaptic Ca^{2+} current and on synaptic transmitter release in the absence of action potentials.

Toxin. Crude venom from American funnel-web spiders, including *Agelenopsis aperta*, *Hololina curta*, and *Calilena*, was obtained commercially (Spider Pharm, Black Canyon, AZ). FTX, a factor with a molecular mass in the 200- to 400-Da range, was purified chromatographically from the venom. We estimate the concentration of toxin used to block Ca^{2+} conductance to be submicromolar, based on the elution profile (OD_{280}) of the FTX fraction on column chromatography and the dilution factors of the chamber.

Affinity Gel Construction. Purified toxin, the activity of which had been previously verified, was coupled to Sepharose 4B via 1,4-butanediol diglycidyl ether. The purified toxin obtained from 100 μl of the *A. aperta* venom was treated with 50 ml of the spacer-attached gel to form the final affinity gel.

Biochemical Methods. *Animals.* Adult Hartley guinea pigs (400–600 g) were decapitated with a small-animal guillotine under sodium pentobarbital (Nembutal, 40 mg/kg, i.p.) anesthesia. A rapid craniotomy was performed to remove the squamous portion of the occipital bone. The cerebellum was then separated from the brainstem and placed in ice-cold 400 mM sucrose/5 mM Tris·HCl, pH 7.4/0.1% phenylmethylsulfonyl fluoride/0.1% bacitracin/5 mM EDTA containing approximately 2 units of aprotinin per ml.

Adult squid (*Loligo Pealeii*) with a 10- to 13-cm mantle size were decapitated, and the optic lobe was excised and rapidly frozen in liquid nitrogen.

Abbreviations: FTX, funnel-web spider toxin; TTX, tetrodotoxin.

Purification Procedure. Published protocols for the affinity purification of membrane proteins (10) were followed for the isolation of the toxin-binding components of the cerebellar and optic lobe membranes. The membrane pellet was resuspended to a concentration of 20 mg of protein per ml into 100 mM sodium citrate, pH 7.4/ 3% sodium choleate to solubilize the membrane protein in a Dounce homogenizer. The solution was stirred overnight at 4°C and centrifuged at 47,000 × *g* for 30 min; the supernatant was filtered under vacuum. The resulting filtrate was then subjected to affinity chromatography. The solution containing the solubilized membrane protein was allowed to react batchwise with 20 ml of the toxin-Sepharose gel by gently stirring overnight at 4°C. The gel was separated from the detergent solution by vacuum filtration. The resulting gel cake was resuspended into 20 ml of 1 M $CaCl_2$/1% sodium choleate/10 mM Hepes, pH 7.4, and was stirred for 2 hr at 4°C. The suspension was then filtered, and the filtrate was retained. The elution procedure was repeated a second time, and the resulting filtrates were combined. The volume of the solution was reduced by dialysis against polyethylene glycol 35,000 (Merck). The protein-containing concentrate was desalted on a 1.0 × 25 cm column of Sephadex G-25 equilibrated with 100 mM Hepes (pH 7.4) and was dialyzed extensively against 400 mM sucrose/10 mM Hepes, pH 7.4. Samples were taken at each step of the procedure for determination of protein by the Bradford assay (11). The product obtained with this procedure typically had a final yield of 0.0005% or less, consistent with the purification of a membrane protein such as an ionic channel.

Ca^{2+}-Channel Reconstitution and Recording. The purified protein was reconstituted into lipid vesicles by using a 4:1 mixture of phosphatidylethanolamine/phosphatidylcholine (Sigma) in 400 mM sucrose formed by the sonication–dialysis procedure of Racker (12, 13). After vesicle formation, the dialysate was applied to a 1.0 × 35 cm column of Sephadex G-25, and the void volume was collected. The resulting vesicle suspension was used for the bilayer studies.

The functional activity of the reconstituted protein was studied by using the lipid bilayer technique. Vesicles containing affinity-gel-processed protein were fused to a planar lipid bilayer, and the electrical activity was determined. Bilayers were formed on two-pull micropipettes with opening diameters near 1 μm by using a lipid solution composed of a 3:1 mixture of phosphatidylcholine/phosphatidylethanolamine (Avanti Polar Lipids). Voltage was applied via the micropipette by using a Dagan 8900 patch/whole-cell clamp with a 10-GΩ head stage (Dagan Instruments, Minneapolis). The bathing solution was held at ground. Data obtained in the channel studies were amplified to a level of 500 mV/pA, and the membrane current was recorded on an HP 3960 FM instrumentation recorder for subsequent analysis. Data were filtered at 1 kHz and were digitized at 2500 or 5000 samples per sec. The digitized records could then be viewed on a computer-generated display, and amplitude and open-time and closed-time distributions were obtained.

RESULTS

The Effect of FTX on the Intact Mouse. The activity of the toxin fraction was tested on mice. The results indicate that for a 30-g mouse, a 5-μl i.p. injection of a solution diluted 1:9 from the spider venom fraction produced death in 15–20 min, apparently by respiratory failure. No effect was observed on neuromuscular transmission. With half of the lethal dose, the animal became sleepy and rarely responded to auditory, visual, or tactile stimuli; when present, the response was phasic and short-lasting, emulating abrupt awakening from deep sleep. The results suggest that FTX crosses the brain–blood barrier, directly affecting the CNS. This is in contrast with results reported for the dihydropyridines (14, 15) and conotoxins (16, 17), which have little effect on mammalian CNS.

The Effect of FTX on Purkinje Cells. Intracellular recordings from Purkinje cells were obtained from cerebellar slices (4, 8). The two types of spike responses typically recorded from these neurons under control conditions are shown in Fig. 1. Depolarization of the neuron by square current pulses produced rapid sodium-dependent firing, which culminated in a set of long, low-amplitude, repetitive Ca^{2+}-dependent spikes (Fig. 1*A*). After bath application of FTX, the Ca^{2+}-dependent spikes disappeared, and the duration of the after-potential hyperpolarization was reduced (Fig. 1*B*). This blocking occurred 5–10 min after bath application of the toxin at a calculated 0.5 μM final concentration and was partly reversible after washing for about 30 min. In addition to blocking the Ca^{2+}-dependent action potentials, FTX increased the likelihood of plateau potentials (Fig. 1*B*), which are produced by the activation of the persistent Na^+ conductance (8, 9). Both of these plateau potentials and the initial fast spikes were blocked by the addition of TTX (10^{-6} g/ml) to the bath (Fig. 1*C*). Nearly identical results were obtained with FTX from the three different types of funnel-web spiders tested.

In a second set of experiments, recordings were made from the Purkinje cell soma after TTX administration. Under these

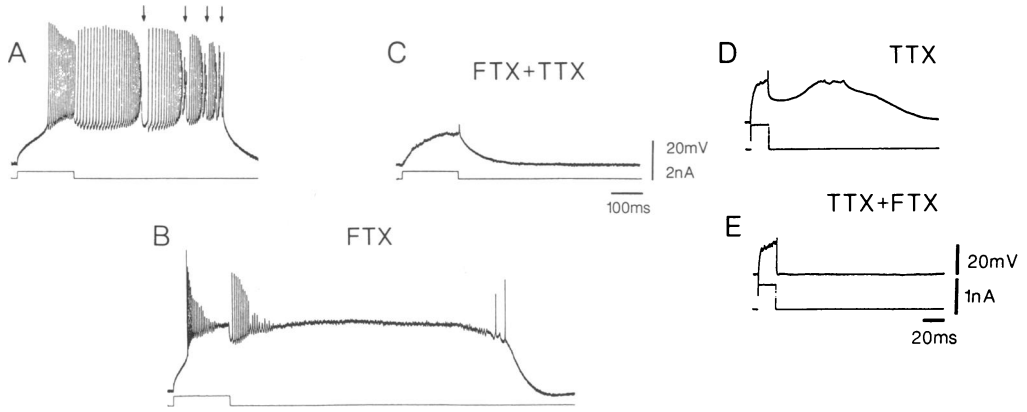

FIG. 1. (*A*) Intracellular recording from a Purkinje cell shows fast Na^+-dependent spikes and Ca^{2+}-dependent action potentials (arrows). (*B*) Five minutes after application of FTX, Ca^{2+} spiking disappeared, and a prolonged Na^+-dependent plateau potential is observed that far outlasts the duration of the stimulation (lower trace). (*C*) Addition of TTX to the bath blocks the fast action potentials and the plateau potentials shown in *B*. (*D*) Ca^{2+}-dependent slow action potential is generated by direct stimulation of the Purkinje cell in the presence of TTX. (*E*) Addition of FTX to the bath produces a blockage of the voltage-dependent Ca^{2+} electroresponsiveness.

conditions, Purkinje cell stimulation is known to elicit a slow Ca^{2+}-dependent plateau potential (8, 9). One such response is illustrated in Fig. 1*D*. In this case, a short, direct depolarization of the soma initiated a prolonged dendritic potential that outlasted the pulse by about 20 msec. However, after application of FTX (≈0.5 μM), this Ca^{2+}-dependent conductance was blocked (Fig. 1*E*).

Single-Channel Properties. The functional activity of the isolated protein was assessed by the lipid-bilayer technique. Electrical activity was measured in asymmetric solutions containing 80 mM $BaCl_2$ and 10 mM Hepes (pH 7.4) on the cis side and 120 mM CsCl, 1 mM $MgCl_2$, and 10 mM Hepes (pH 7.4) on the trans side or in the patch pipette. Recordings were also obtained with the solutions reversed. When vesicles containing the purified protein were added to the bilayer chamber, an increase in the conductance of the bilayer was usually detected within 10 min. In general, it was difficult to obtain recordings of only a single channel when vesicles were added to the Ba^{2+}-containing solutions because of the fusion-promoting effect of divalent cations.

Two types of single-channel activity were found. The first was seen when Ba^{2+} was present on the extracellular face of the channel protein and was characterized by short-duration openings. Fig. 2 *A–C* illustrates this activity from the cerebellar preparation at holding potentials of −45, −30, and −15 mV. The voltage dependence of the open probability is shown in Fig. 2*F*. The channel was closed at −60 mV and began to exhibit openings as depolarizing potentials were applied. The maximum open probability, 0.6–0.65, occurred at holding potentials greater than 0 mV. The mean open time was also found to be voltage-dependent and ranged from less than 0.6 msec to 5 msec. The *I–V* relationship constructed from six experiments is nonlinear as shown in Fig. 2*E*, where each point represents the mean of the current at each voltage step. Voltage steps above 0 mV generated unitary currents too low to be measured reliably (Figs. 2*E* and 4 *F* and *G*). A conductance of 10–12 pS in Ba^{2+} and 6–8 pS in 100 mM Ca^{2+} was obtained from these data. The extrapolated reversal potential was between −90 and −120 mV, which, to the limit of the accuracy of the measurements, is the theoretical value for a Ba^{2+} permeable channel.

A second type of channel-like activity was found when the solutions were reversed so that the high-Ba^{2+} solution was on the cytoplasmic face of the channel. Typical recordings are shown in Fig. 2*D*, which were made at holding potentials of −45, −30, and −15 mV. In this particular experiment, three channels with identical conductances had fused with the bilayer. An unexpected characteristic was the predominance of openings longer than 1 sec. Also present are rapid openings with durations of less than 100 msec. From these data we estimated a unitary channel conductance of 20 pS.

The measured Ca^{2+} currents represent contributions from both the individual currents and the opening probabilities of the channels. Thus, it should be possible to approximate the macroscopic current by multiplying the single-channel currents by the opening probabilities at each potential as has been done for the "fast" Ca^{2+} channel (18). The voltage and time dependence of the current obtained in this way is comparable to the results from current clamp experiments in the dendrites of Purkinje cells (8). However, in the absence of Ca^{2+}-current measurements for Purkinje cell dendrites, only a qualitative statement can be offered. The effect of known blockers of the neuronal Ca^{2+} channels was determined for the reconstituted channels. Single channels were blocked by both Cd^{2+} and Co^{2+} at concentrations of less than 100 μM in a manner consistent with a fast-block mechanism (18). The single channels were also blocked by the microliter addition of a 1:10 dilution of FTX.

Cephalopod Ca^{2+} Channels. A set of experiments similar to those described for the Purkinje cell were carried out at the squid giant synapse. Two experimental paradigms were followed. Pre- and postsynaptic intracellular recordings were obtained, and synaptic transmission was tested by electrical activation of the presynaptic fiber. Presynaptic stimulation generated a presynaptic action potential that served as a trigger for transmitter release and the generation of a postsyn-

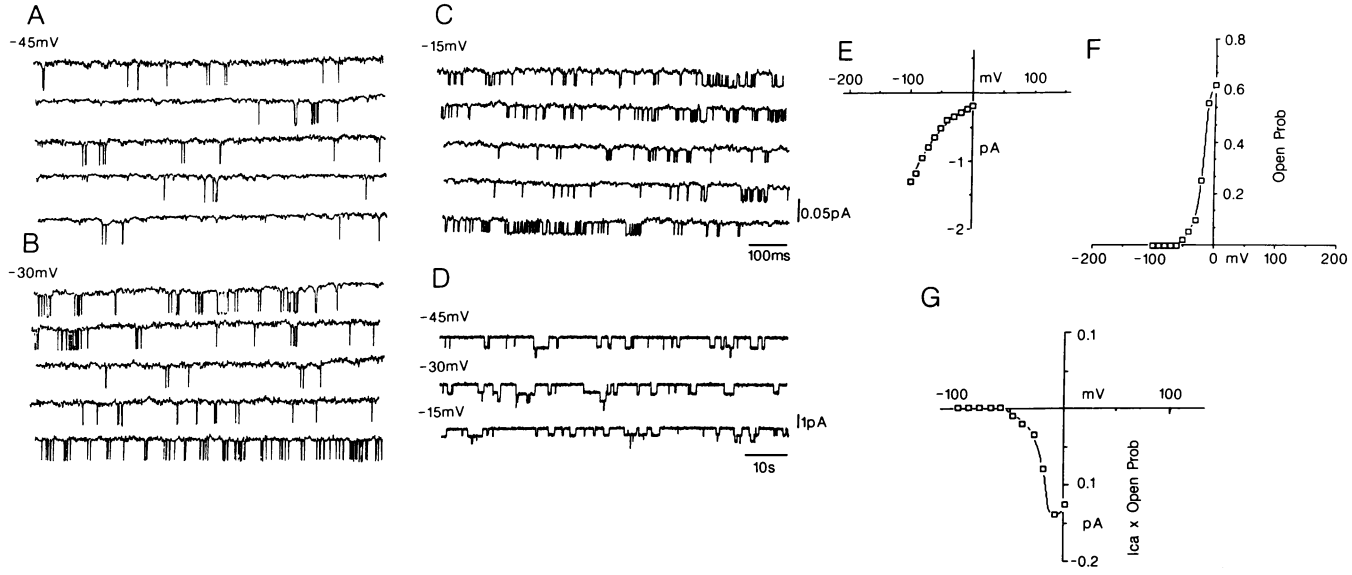

FIG. 2. Functional properties of channels isolated from guinea pig cerebellum by an FTX affinity gel. (*A–C*) Single-channel recording with 80 mM external Ba^{2+} obtained for protein reconstituted in lipid vesicles and fused with lipid bilayer. Holding potentials: −45 mV (*A*), −30 mV (*B*), and −15 mV (*C*). (*D*) Single-channel recordings obtained with 80 mM Ba^{2+} on the cytoplasmic face of the channel. Holding potentials of −45, −30, and −15 mV are shown. In this particular experiment, three identical channels had fused with the bilayer. The long duration of the open time seems to be an effect of the high amount of internal Ba^{2+}, as it can be converted into the short-duration channel (*A–C*) when Ba^{2+} is removed from the cytoplasmic side. (*E*) *I–V* curve in 80 mM Ba^{2+} for the "fast" channel of *A–C* constructed from the single-channel events obtained from six different experiments. Each point represents the mean current from 200 or more events at each voltage. (*F*) Plot of open probability vs. applied voltage showing the voltage dependence of the channel, which reaches a maximum value of 0.6–0.65 above 0 mV. (*G*) Values from *E–F* multiplied to give an approximation of the macroscopic current.

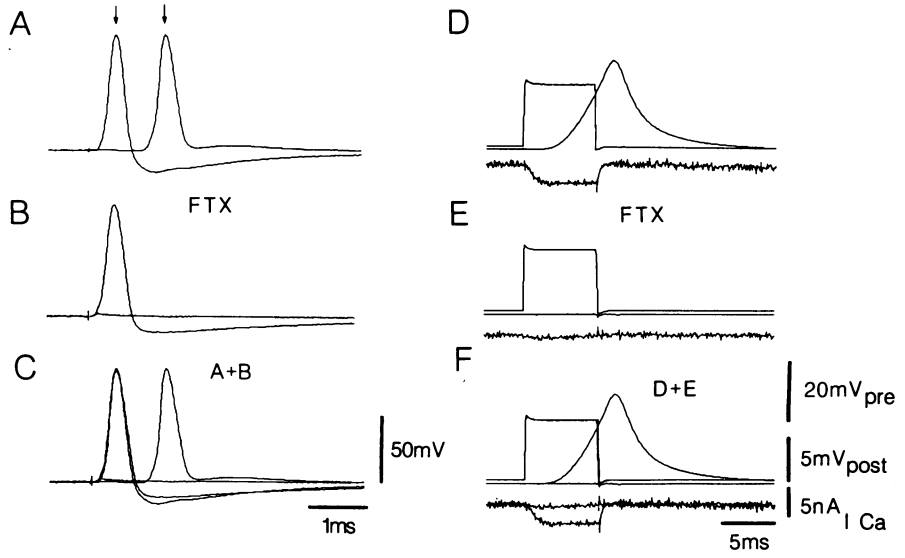

FIG. 3. Action of FTX on synaptic transmission at the squid giant synapse. (*A–C*) Effect of FTX on synaptic transmission evoked by presynaptic action potentials. Pre- (first arrow) and postsynaptic (second arrow) action potentials were evoked after direct stimulation of the preterminal fiber (*A*). Five minutes after the application of FTX, a total block of synaptic transmission was observed without affecting significantly the presynaptic action potential (*B*). Superimposition of the records in *A* and *B* (*C*) shows the small reduction in the amplitude of the afterpotential hyperpolarization after application of FTX. (*D–F*) Presynaptic voltage-clamp records and postsynaptic recording. Traces: upper, voltage step; middle, postsynaptic response; lower, inward calcium current. Results are shown before (*D*) and 10 min after (*E*) the application of FTX. Note the block of the calcium current and the postsynaptic response. Superimposition of records in *D* and *E* is shown in *F*.

aptic response (Fig. 3*A*). After administration of FTX in submicromolar concentrations, synaptic transmission was blocked within 5–8 min, and the presynaptic afterpotential hyperpolarization was slightly reduced (Fig. 3*B*). In a second set of experiments, the presynaptic terminal was voltage-clamped, and the relation between the presynaptic Ca^{2+} current and transmitter release was studied as shown in Fig. 3*D*. Addition of FTX at similar concentrations to that used in the experiment illustrated in Fig. 3*E* blocked the Ca^{2+} current within a few minutes. This was accompanied by a block of transmitter release, as judged by the absence of a postsynaptic response. The toxin fraction did not have a direct effect on postsynaptic channels, since no reduction of the postsynaptic response to pressure-injected glutamic acid was observed after the synaptic transmission was blocked by the toxin (not shown).

Isolation of Ca^{2+} Channels from the Squid Optic Lobe. Channel protein derived from the optic lobe was extracted and studied in the black lipid membranes. In Fig. 4 examples of the single-channel currents are illustrated. In the same asymmetric solutions used for the cerebellum, two types of channel-like activity were found. The first, shown at three holding potentials in Fig. 4 *A–C* was characterized by voltage-dependent openings with a mean duration of 1–3

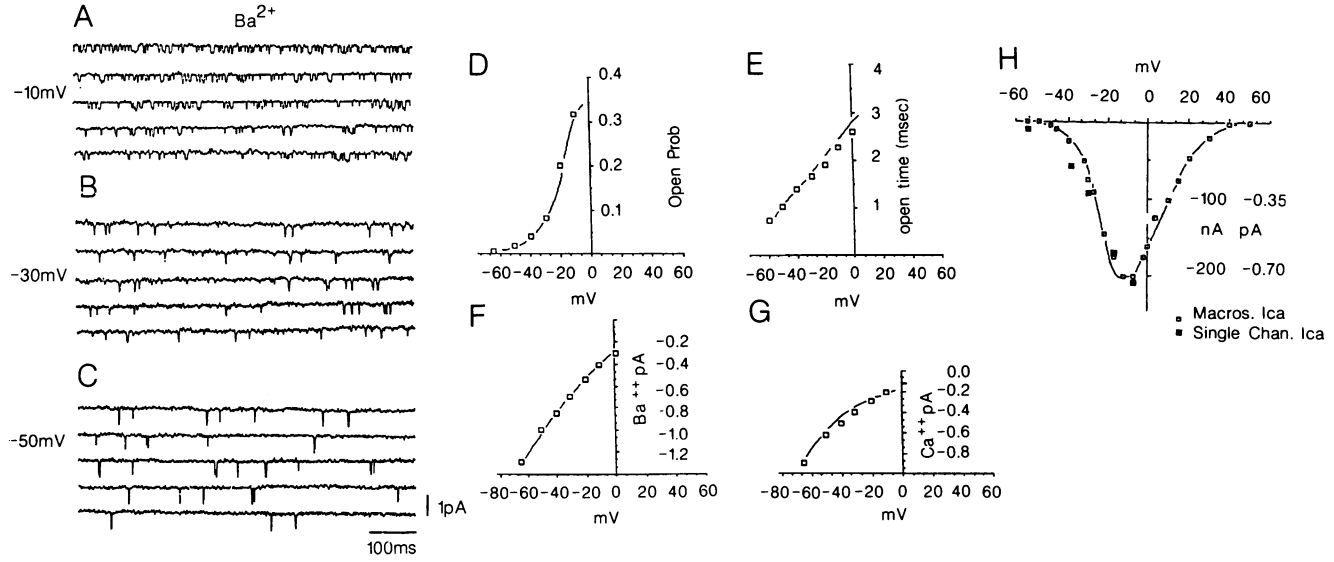

FIG. 4. Single-channel properties of protein from squid optic lobe. (*A–C*) Single-channel recordings at potentials of −10, −30, and −50 mV were obtained with 80 mM Ba^{2+} on the external face of the protein. (*D*) Opening probability of the channel reaches a maximum of 0.32–0.35 at 0 mV and above, exhibiting a clear voltage dependence ($n = 6$). (*E*) Mean open time vs. potential shows the voltage dependence of the length of time the channel remains open as the holding potential is varied ($n = 6$). (*F* and *G*) *I–V* curves obtained in 80 mM Ba^{2+} (*F*) and 100 mM Ca^{2+} (*G*). The conductance of the channel is 20 pS in Ba^{2+} and 8 pS in Ca^{2+} (200+ events at each potential). (*H*) □, Current obtained by multiplying values in *D* and *G* to approximate macroscopic behavior; ■, actual values for I_{Ca} in squid as previously published (9).

msec (Fig. 4*E*). The unitary conductance of the channel was 18–20 pS in 80 mM Ba^{2+} (Fig. 4*F*) and 5–8 pS in 100 mM Ca^{2+} (Fig. 4*G*). The opening probability, which was also voltage-dependent, reached a maximum of 0.35 at a membrane potential of 0 mV. When the cytoplasmic face of the protein was exposed to high-concentration Ba^{2+} solutions, long open times of the channel were induced, and replacement of the Ba^{2+} ions on the cytoplasmic side with Cs^{+} resulted in conversion of the long openings to short openings. High concentrations of internal Ca^{2+} (100 mM) did not induce the long open times. As both the probability of opening and the single-channel current are dependent on voltage, multiplication of these two parameters would give the current–voltage relationship for the macroscopic current. Such a plot for the fast channel, as shown in Fig. 4*H*, is quite similar to the macroscopic I_{Ca} recorded from the squid preterminal (19, 20).

Results similar to those determined for the cerebellar channel were found in the channels from squid optic lobe. Both long-duration and short-duration opening time were recorded. The squid fast channel differed from the cerebellar channel in two respects. First, the conductance of the squid channel was higher. The *I–V* curve constructed from a series of experiments on the short-duration channel is shown in Fig. 4 *F* and *G*. The unitary conductance was estimated to be 20 pS. A second difference between the two channels is that the cerebellar channel has a 2-fold higher maximum probability of opening. However, the voltage-dependence of the channels and their pharmacological characteristics are quite similar.

DISCUSSION

The present paper indicates that FTX, a fraction of funnel-web spider poison having a molecular mass of 200–400 Da, blocks Ca^{2+} channels both in mammalian Purkinje cells and at the presynaptic terminal of the squid giant synapse. Because this channel has unique pharmacological properties and kinetics that are somewhat different from those described for the L, N, and T channels (2, 3), we propose that it should be referred to as the "P" channel, since it was first described in Purkinje cells. Whether the P channel observed in Purkinje cells and in the squid giant synapse are indeed the same is difficult to say at this time. From an electrophysiological point of view, the macroscopic Ca^{2+} currents obtained from presynaptic voltage clamp studies (18, 19) and those obtained from black lipid membrane recordings of channels isolated from cerebellum show a similar *I–V* relation. Because reliable voltage-clamping of Purkinje cells so far has not been technically feasible, we cannot compare the computed *I–V* relation obtained from single Ca^{2+}-channel recordings with macroscopic I_{Ca}. However, the similarity between the kinetics of those observed in squid and Purkinje cells suggests that these two channels are similar.

A comparison of the P channel with previously described Ca^{2+} channels (2, 3) indicates clear differences. Indeed, the electrophysiological properties of both the squid giant synapse presynaptic spike as well as the action potential recorded from Purkinje cell dendrites are quite different from the low-threshold calcium spike observed in central neurons (20), which corresponds to the activation of the T channels (2, 3). Neither can the P channel be considered to be similar to the L channel, since the voltage-dependence of this channel is far more negative (−60 mV) (19, 20) than that reported for the L channel (2, 3). In addition, at least in the squid presynaptic terminal, a degree of inactivation may be observed. If anything, our channel may resemble the N channel. However, the P channel is not blocked by ω-conotoxin. In short, we must conclude on pharmacological and electrophysiological criteria that there exists yet another Ca^{2+} channel. This P channel is, in our estimation, one of a large variety of Ca^{2+} channels that will probably be encountered in the years to come.

In addition to the differences in pharmacology, single-channel conductances, and voltage-dependence kinetics, it is possible that the different channels have fundamentally different properties from a biochemical point of view as well. One of the interesting aspects of the present results relates to the action of calmodulin kinase II (CAMkinase II) on Ca^{2+} channels. This enzyme is known to phosphorylate the L-type Ca^{2+} channels, increasing their average open times, resulting in an increased Ca^{2+} current when these channels are phosphorylated (21). In the squid giant synapse, presynaptic injection of CAMkinase II has been shown to increase transmitter release as much as 7-fold without an observable effect on the Ca^{2+} current (22), indicating that CAMkinase II may modulate transmitter release by phosphorylation of synapsin I at site 2 (23, 24), which would increase vesicular availability at the presynaptic release site (22). Thus, specific biochemical modulation of the different Ca^{2+} channels may be a fundamental variable in their role in nervous system function.

This work was supported by National Institute of Neurological and Communicative Disorders and Stroke Grants NS13742 and AFOSR85-0368.

1. Tsien, R. W., Lipscombe, D., Madison, D. V., Bley, K. R. & Fox, A. P. (1988) *Trends NeuroSci.* **11,** 431.
2. Fox, A. P., Nowycky, M. C. & Tsein, R. W. (1987) *J. Physiol. (London)* **394,** 149–172.
3. Fox, A. P., Nowycky, M. C. & Tsien, R. W. (1987) *J. Physiol. (London)* **394,** 173–200.
4. Sugimori, M. & Llinás, R. (1987) *Soc. Neurosci. Abst.* **13.**
5. Tank, D. W., Sugimori, M., O'Connor, J. A. & Llinás, R. (1988) *Science* **242,** 773–777.
6. Sugimori, M., Lin, J. W., Cherksey, B. & Llinás, R. (1988) *Biol. Bull.* **175,** 308.
7. Cherksey, B., Sugimori, M., Lin, J. W. & Llinás, R. (1988) *Biol. Bull.* **175,** 304.
8. Llinás, R. & Sugimori, M. (1980) *J. Physiol. (London)* **305,** 171–195.
9. Llinás, R., Steinberg, I. Z. & Walton, K. (1981) *Biophys. J.* **33,** 289–322.
10. Cherksey, B. D. (1988) *J. Comp. Physiol. Biochem.* **90A,** 771–773.
11. Bradford, M. (1976) *Anal. Biochem.* **12,** 248–254.
12. Racker, E., Knowles, A. F. & Eytan, E. (1975) *Ann. N.Y. Acad. Sci.* **264,** 17–33.
13. Cherksey, B. D. & Zeuthen, T. (1987) *Acta Physiol. Scand.* **129,** 137–138.
14. Fleckenstein, A. (1977) *Annu. Rev. Pharmacol. Toxicol.* **17,** 149–166.
15. Weiss, G. B., ed. (1981) *New Perspectives on Calcium Antagonists* (Am. Physiol. Soc., Bethesda, MD).
16. Gray, W. R., Luque, A., Olivera, B. M., Barret, J. & Cruz, L. J. (1981) *J. Biol. Chem.* **256,** 4734–4740.
17. Olivera, B. M., McIntosh, J. M., Cruz, L. J., Luque, F. A. & Gray, W. R. (1984) *Biochemistry* **23,** 5087–5090.
18. Hille, B. (1984) *Ionic Channels of Excitable Membranes* (Sinauer, Sunderland, MA).
19. Llinás, R., Steinberg, I. Z. & Walton, K. (1981) *Biophys. J.* **33,** 323–352.
20. Llinás, R. (1988) *Science* **242,** 1654–1664.
21. Armstrong, D. (1988) *J. Gen. Physiol.* **92,** 10a (abstr.).
22. Llinás, R., McGuinness, T. L., Leonard, C. S., Sugimori, M. & Greengard, P. (1985) *Proc. Natl. Acad. Sci. USA* **82,** 3035–3039.
23. DeCamilli, P., Cameron, R. & Greengard, P. (1983) *J. Cell Biol.* **96,** 1337–1354.
24. Huttner, W. B., Schiebler, W., Greengard, P. & DeCamilli, P. (1983) *J. Cell Biol.* **96,** 1374–1388.